Available online at www.sciencedirect.com
ScienceDirect
Vibrational Spectroscopy 43 (2007) 140–151
VIBRATIONAL SPECTROSCOPY
www.elsevier.com/locate/vibspec

Hydration effects on the molecular structure of silica-supported vanadium oxide catalysts: A combined IR, Raman, UV–vis and EXAFS study

Daphne E. Keller, Tom Visser, Fouad Soulimani, Diek C. Koningsberger, Bert M. Weckhuysen *

Inorganic Chemistry and Catalysis, Department of Chemistry, Utrecht University, P.O. Box 80083, 3508 TB Utrecht, The Netherlands

Received 18 April 2006; received in revised form 7 July 2006; accepted 7 July 2006
Available online 22 August 2006

Abstract

The effect of hydration on the molecular structure of silica-supported vanadium oxide catalysts with loadings of 1–16 wt.% V has been systematically investigated by infrared, Raman, UV–vis and EXAFS spectroscopy. IR and Raman spectra recorded during hydration revealed the formation of V–OH groups, characterized by a band at 3660 cm^{-1}. Hydroxylation was found to start instantaneously upon exposure to traces of water, reflecting a very high sensitivity of the supported vanadium oxide catalysts for H_2O. Further hydration resulted in the appearance of a V–O–V vibration band located around 700 cm^{-1} pointing to the formation of di- or polymeric species. EXAFS analysis at 77 K indicated structural changes as the oxygen coordination changed from four to five. Moreover, a V···V contribution was detected for the hydrated species. The IR, Raman and UV–vis data suggested a pyramidal anchoring of the dehydrated VO_x species, whereas, the EXAFS data pointed to the presence of single V–O–Si bonded VO_x species. This difference is attributed to water condensation effects at 77 K during EXAFS acquisition, resulting in a partial re-hydroxylation of the dehydrated samples, as confirmed by complementary IR and Raman analysis. Combining the results of this study with data from our previous studies [D.E. Keller, F.M.F. de Groot, D.C. Koningsberger, B.M. Weckhuysen, J. Phys. Chem. B 109 (2005) 10223; D.E. Keller, D.C. Koningsberger, B.M. Weckhuysen, J. Phys. Chem. B 110 (2006) 14313] as well as literature led to a reaction scheme in which a monomeric VO_x species anchored by three Si–O–V bonds to the silica support (pyramidal-type structure) is transformed into a monomeric VO_x species anchored by one Si–O–V bond (umbrella-type structure) by partial hydration of the catalyst material. This results in the formation of both V–O–H and Si–O–H bonds. At higher water pressures, larger vanadium oxide clusters are formed due to full hydration of the catalyst surface and a de-attachment of the vanadium oxide from the support surface. The results of this study provide evidence, that an umbrella-type structure (*i.e.*, Si–O–V=O$(OH)_2$) could be present under catalytic conditions where H_2O is a reaction product (*e.g.*, partial oxidation of methanol to formaldehyde and oxidative dehydrogenation of alkanes). In other words, both the pyramidal ((Si–O)$_3$–V=O) and the umbrella (Si–O–V=O$(OH)_2$) model can exist at a support surface, their relative ratio depending on the hydration degree of the catalyst material. This study also illustrates that a corroborative characterization requires the use of multiple spectroscopic techniques applied at the same samples under almost identical measuring conditions.

Keywords: Supported VO_x; Influence hydration; SiO_2; XAFS; Raman/IR; UV/vis spectroscopy

1. Introduction

Supported vanadium oxide catalysts are of great interest because of their high potential in a wide variety of oxidation reactions [1–7]. A key step to fully understand the catalytic working mechanism is a profound knowledge of the molecular structure of the vanadium oxide (VO_x) under reaction conditions and the way it is anchored at the surface of the support material. The latter is of importance in order to better understand vanadium oxide-support effects. For these reasons, the molecular structures of supported VO_x on a variety of support materials, under various conditions and over a broad range of vanadium oxide loadings have been the subject of many spectroscopic studies including IR [8–15], Raman [15–24], UV–vis-NIR [25–29] and EXAFS [30–36].

The molecular structure of the hydrated supported vanadium oxide catalysts can also be of interest for a better understanding of their catalytic performances. H_2O for instance, is formed during some oxidation reactions, which may lead to a partial hydration of the catalyst surface [37]. Seminal examples

* Corresponding author. Tel.: +31 30 2534328.
E-mail address: b.m.weckhuysen@chem.uu.nl (B.M. Weckhuysen).

0924-2031/$ – see front matter
doi:10.1016/j.vibspec.2006.07.005

include the selective oxidation of methanol to formaldehyde and the oxidative dehydrogenation of propane to propene. The extent of catalyst hydration, the vanadium oxide loading and the type of support oxide are known to influence the molecular structure of the vanadium oxides under ambient and hydrated conditions, although crystalline V_2O_5 species are reported to be usually unaffected by water vapor [37]. The hydration process of silica-supported vanadium oxide catalysts has been described by Gao et al. [38]. Upon hydration the vanadium species is supposed to go through a series of subsequent stages, *i.e.*, hydrolysis of a V–O–Si bond, addition of water, formation of oligomers, formation of chain polymers, formation of 2D polymers and finally the formation of a 2D layered structure ($V_2O_5{\cdot}nH_2O$) [38]. The formation of V–OH groups upon hydrolysis of V–O–Si bridging bonds has also been proposed by several other groups, mainly based on the appearance of a (V–)O–H stretching band at 3660 cm^{-1} in the vibrational spectra [13,39–43]. Berndt et al. [39] observed this band after treatment with steam at 600 °C, whereas, Nguyen et al. [40] reported its presence even at dehydrated conditions. Others recorded the band in the spectra of hydrated samples at room temperature [13,41–43]. An extensive Raman spectroscopic study on the effect of water vapor on the molecular structures of supported vanadium oxide catalysts at different temperatures has been carried out by Jehng et al. [37]. For VO_x/SiO_2 changes in the Raman spectrum between 1200 and 100 cm^{-1} were not observed. Unfortunately, potential hydration effects were not discussed in detail, as inferred from the fact that the OH stretching region was not reported in the paper.

Hazenkamp and Blasse [44] suggested for their silica-supported vanadium oxide catalyst, that vanadium oxides are present as decavanadates when hydrated, while Yoshida et al. concluded the coordination of vanadium to be octahedral on the basis of an NMR analysis of hydrated vanadia nanoparticles on titania [45], Nielsen et al. [46] concluded that vanadium was six coordinated with one short (V=O) and one long (V–O) axial bond. Silversmit et al. [36] used EXAFS to determine the structure of a 2.8 wt.% vanadium on titania catalyst. They found a V_2O_5 resembling octahedral coordination with one short V=O bond of 1.6 Å, four longer V–O bonds of 2 Å and one long V–O bond of 2.2 Å. Ruitenbeek et al. [30,31,47] came to the conclusion on the basis of EXAFS that for a hydrated 17.5 wt.% alumina-supported catalyst the vanadium was four coordinated with one V=O bond of 1.55 Å, one V–OH bond of 1.74 Å and two V–O bonds of 1.90 Å. A similar molecular structure has been suggested for 1.4 wt.% vanadium on alumina, silica and titania by Went et al. [48].

In general, the molecular structure of VO_x species in aqueous environment, for example, present in fully hydrated catalysts, is dictated by the concentration of the vanadium oxide species and the pH of the water layer on top of the support surface, which in turn is determined by the point of zero charge (PZC) of the support oxide [49]. The relation between the vanadium oxide concentration, the pH of the solution and the resulting molecular structure of the vanadium oxide species is illustrated in the so-called predominance diagrams [50]. Based on such diagrams and the PZC of the support oxide, Wachs and co-workers proposed that upon hydration, silica-supported vanadium oxide catalysts consist of a mixture of V_2O_5, $V_{10}O_{26}(OH)_2$ and $VO(OH)_3$ for low loading and $V_{10}O_{26}(OH)_2$ and V_2O_5 for high vanadium oxide loading [49,51–53].

More detailed information is available in the literature about the molecular structure of supported vanadium oxide under dehydrated conditions. It is commonly agreed that vanadium oxide can be present on the support oxide in three different forms, *i.e.*, as monomeric VO_4 species at low loadings (typical < 2.3 VO_x nm^{-2}), in a polymeric form at medium loadings (2.3–7.5 VO_x nm^{-2}) and as V_2O_5 crystals at high loadings (>7.5 VO_x nm^{-2}) [54]. There is, however, still no consensus on the precise geometrical molecular structure of the different forms. Of particular interest and renewed subject of debate is the molecular structure of the supported low loaded monomeric VO_4 species under dehydrated conditions. The origin of this revived debate is related to uncertainties about specific spectral assignments in the vibrational spectra as illustrated by studies of Magg et al. [55,56] and Gijzeman and co-workers [57,58]. As depicted in Fig. 1, three different possibilities have been suggested in the literature for the way the monomeric VO_4 species is anchored at the support oxide under dehydrated conditions: (a) via two support oxygen bonds with as a consequence a di-oxo structure, (b) via three support oxygen bonds with a single V=O bond, and (c) via one support oxygen bond, a single V=O bond and a peroxo group. Furthermore, other species (d) and (e) are proposed to be formed under various measurement conditions.

The di-oxo structure (a) is commonly rejected based on the results of EXAFS analysis [30–33] and the absence of a symmetric and anti-symmetric V=O stretching band in the vibrational spectra [59–61]. The single V=O nature of the VO_4 unit has been confirmed with ^{18}O labeling experiments in conjunction with Raman spectroscopic analysis [60,61]. As a consequence, structure (b) with one V=O bond pointing upwards and three V–O-support bonds downwards has been most generally accepted as the correct geometry [62–66]. However, recent EXAFS studies at 77 K on low-loaded

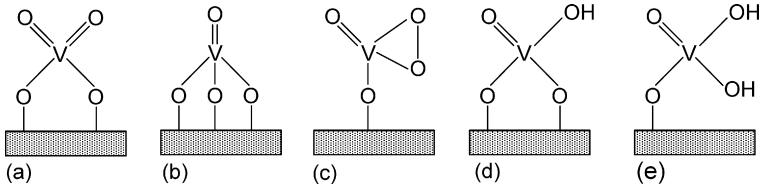

Fig. 1. Possible molecular structures of monomeric VO_4 species on a silica support.

supported vanadium oxide species on alumina, silica, niobia and zirconia after dehydration in combination with structural models of the support-vanadium oxide interface, pointed to only one V–O_b–$M_{support}$ bond, one V=O bond and two other V–O bonds, thus giving support for either the structure (c) or (e), EXAFS being unable to detect either potential hydrogen atoms near the vanadium scatterer or a bond between the O atoms [32,33]. On the other hand, it was suggested, on the basis of DFT calculation and temperature dependent Raman spectra that the observed band at 915 cm^{-1} might originate from a perturbed peroxide O–O stretching vibration [57,58]. Interestingly, it has been shown that the band is also present in catalysts with a low vanadium oxide loading (1–2 wt.%) in which only monomeric vanadium oxide species are supposed to present [32,58]. EXAFS analysis endorsed the absence of V–O–V bonds at these low loadings, which ruled out that the 915 cm^{-1} band originates from a di- or polymeric species [32,33]. This is in line with conclusions of Wu et al. [67] from UV-laser Raman analysis of VO_x/alumina catalysts. These authors concluded that the 915 cm^{-1} Raman shift is particularly present at lower loading and they assigned the band to a V–O-support vibration.

The aim of the research described in this paper was to determine the influence of the degree of hydration on silica-supported vanadium oxide catalysts, in order to obtain a more consistent picture of the geometrical orientation of the VO_x species and its interfacial geometry. More specifically, we were interested to determine the viability of either structure (c) and (e) as a potential vanadium oxide species at support surfaces. For this purpose, a series of VO_x/SiO_2 catalysts with loadings between 1 and 16 wt.% VO_x have been investigated. The samples were characterized with IR, Raman and UV–vis spectroscopy under dehydrated, partially hydrated and fully hydrated conditions. Complementary EXAFS measurements were carried out on the 1 wt.% VO_x/SiO_2 catalyst samples.

2. Experimental

2.1. Catalyst preparation

A series of six well-defined supported vanadium oxide catalysts with increasing vanadium oxide loading were prepared using SiO_2 (home made, pore volume of 0.70 ml g^{-1} 1 and surface area of 600 m^2 g^{-1}) as support oxide. The SiO_2 support was prepared *via* the sol–gel method according to a slightly altered literature recipe [68], HNO_3 was used instead of HCl. The catalysts were prepared with the incipient wetness impregnation technique using a NH_4VO_3 (Merck, p.a.) solution with oxalic acid (Brocacef, 99.25% pure). The catalysts were dried at room temperature for one night, one night at 393 K and after this treatment they were calcined at 773 K for 3 h. Dehydration was carried out under a stream of O_2 (40 ml min^{-1}) at 700 K for 3 h. The loading of the catalysts corresponds to about 1, 2, 4, 8, 12 and 16 wt.% of vanadium. The samples under investigation are listed together with the catalyst code that will be used throughout the paper in Table 1. In this table, the VO_x coverage per nm^2 compared to the theoretical monolayer for monomers (2.3 VO_x nm^{-2}) as described by Khodakov et al. [54] has been included.

Table 1
Supported vanadium oxide catalysts under investigation with sample code, vanadium oxide loading, surface density and surface monolayer coverage

Sample code	wt.% V	VO_x (nm^{-2})	% of monolayer coverage reached
1V–Si	1.05	0.118	5.1
2V–Si	2.08	0.236	10.3
4V–Si	4.05	0.470	20.4
8V–Si	8.33	1.011	43.9
12V–Si	12.90	1.648	71.6
16V–Si	16.40	2.183	94.9

2.2. Spectroscopic characterization

IR, Raman and UV–vis analysis of the dehydrated samples, including the bare support material, were carried out under a flow of O_2 (40 ml min^{-1}) at 700 K. Spectra of fully hydrated samples were scanned at ambient conditions. Time-resolved IR and Raman measurements were carried out during rehydration by slow diffusion of ambient air into the reactor during cooling down to ambient temperature until rehydration was completed. Additional Raman measurements were carried out at 700 K under vacuum to determine the presence of thermally instable peroxide species (c). For Raman, a special cell with a quartz window was used on which details can be found elsewhere [69]. Raman spectra were collected with a Kaiser RXN spectrometer equipped with a 532 nm diode laser (output power of 60 mW) and a Peltier cooled Andor CCD camera for detection. A 5.5 non-contact objective was used for beam focusing and collection of scattered radiation. Spectra were obtained at CCD exposure times between 10–50 and 20–50 s accumulations were applied to obtain sufficient signal-to-noise ratio. IR measurements were carried out in transmission mode on self-supporting wafers in a glass in situ cell with KBr windows and in diffuse reflectance (DRIFT) mode in a Harrick Praying Mantis DRIFT accessory equipped with an environmental cell. For DRIFT measurements, the sample material was mixed with KBr in a 5/95 ratio mix. All spectra were recorded at a data point resolution of 2 cm^{-1} on a Perkin-Elmer 2000 FTIR spectrometer with DTGS detector. Two scans were co-added for the time-resolved spectra and 100 for all other IR data. Additionally, IR and Raman spectra of self-supported wafers of the 2V–Si and 4V–Si catalysts after dehydration at 700 K were recorded at 77 K in the cell used for EXAFS measurements, to determine possible hydroxylation effects as result of water condensation.

UV–vis diffuse reflectance measurements of the dehydrated samples were carried out in the previously mentioned quartz reaction cell, at room temperature on a Cary 500 UV–vis instrument (Varian) in the range 200–800 nm. Scans were performed with a data interval of 1 nm and a scan rate of 600 nm min^{-1}. A white Halon standard was used as a reference background.

EXAFS analysis has been carried only on the 1V–Si samples as it ideally works for catalytic systems containing a single type

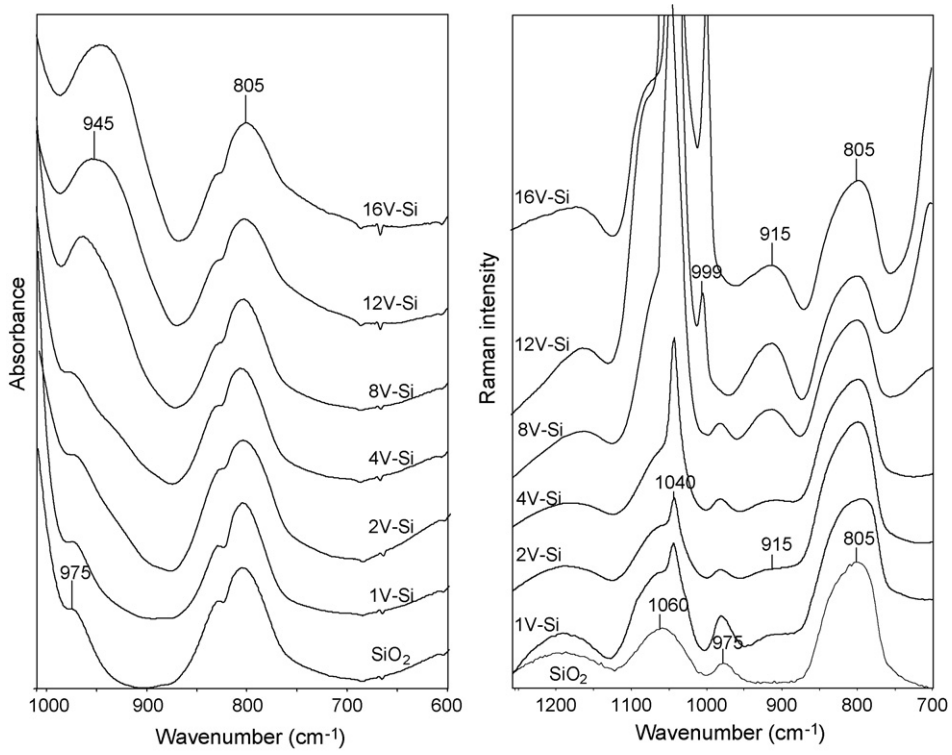

Fig. 2. Diffuse reflectance IR spectra (left) and Raman spectra (right) of dehydrated VO_x/SiO_2 catalysts with loadings from 1 to 16 wt.% V recorded at 700 K.

of surface species. Experiments were carried out at beamline E4 in Hasylab (Hamburg, Germany) using a Si (1 1 1) monochromator. The measurements were performed in fluorescence mode, using an ion chamber filled with 400 mbar N_2 to determine I_0. The detector was a seven-element solid-state (SiLi) detector. The monochromator was detuned to 80% of the maximum intensity at the V K-edge (5465 eV) to minimize the presence of higher harmonics. Measurements were carried out in a cell with Kapton windows on which details can be found elsewhere [70]. Data were collected at 77 K after dehydration (623 K for 2 h in 2.5% O_2/He, 100 ml min^{-1}). XAFS data analysis was carried out using the XDAP code developed by Vaarkamp et al. [71]. The background was subtracted employing cubic spline routines with a continuously adjustable smooth parameter [72]. This led to the normalized oscillatory part of the XAFS data, for which all the contributions to the spectrum, including the AXAFS, were maximized [72]. The fit procedure has been described in detail elsewhere [32,72]. Structural models for the SiO_2 surface were constructed using the CERIUS 2 molecular modeling software [73]. A VO_4 unit was anchored to the support surface and the resulting model was used as auxiliary to determine EXAFS input parameters for fitting the higher coordination shells. The final higher shells EXAFS fits were obtained after several iteration steps with the structural model obtained from CERIUS 2. The (1 1 1) surface of β-quartz gave the best description of the interfacial geometry [33] and this structure was taken from the CERIUS 2 database. To obtain the CERIUS 2 model, the V=O and the V–O distances were set according to the results obtained from the EXAFS analysis including V=O, V–O and V···Si distances. Rotation of the molecule around the Si–O bond and bending of the V–O–Si bond were the only performed operations to find a suitable configuration of the molecule on top of the surface, where the V···Si distance was used as structural constraint. An energy minimization was not performed. The final EXAFS fits were determined after several iteration steps with the structural model obtained from CERIUS 2. Distances to neighboring atoms were determined for the VO_4 cluster on top of β-SiO_2 (1 1 1).

3. Results

3.1. IR and Raman spectroscopy

3.1.1. Dehydrated samples

The IR and Raman fingerprint region of the dehydrated VO_x/SiO_2 samples and the support are shown in Fig. 2. To facilitate comparison, the IR spectra have been normalized on the SiO_2 band at ∼805 cm^{-1}. The same band has been used for normalization of the Raman spectra, but here the result is less reliable as Raman scattering from the quartz reactor window could not be completely filtered out. Other silica support vibrations are found at 1010 and 975 cm^{-1} (IR) and 1175, 1060 and 975 cm^{-1} (Raman). The band at 975 cm^{-1}, which is usually assigned to a Si–O(H) stretching vibration [42] disappears at higher vanadium oxide loadings (>8 wt.%). This can be explained by the increasing consumption of Si–O–H groups by anchoring VO_x species. The IR spectra also show a broad band around 945 cm^{-1} at high vanadium oxide loadings (8–16 wt.%). Spectral subtraction of the support spectrum

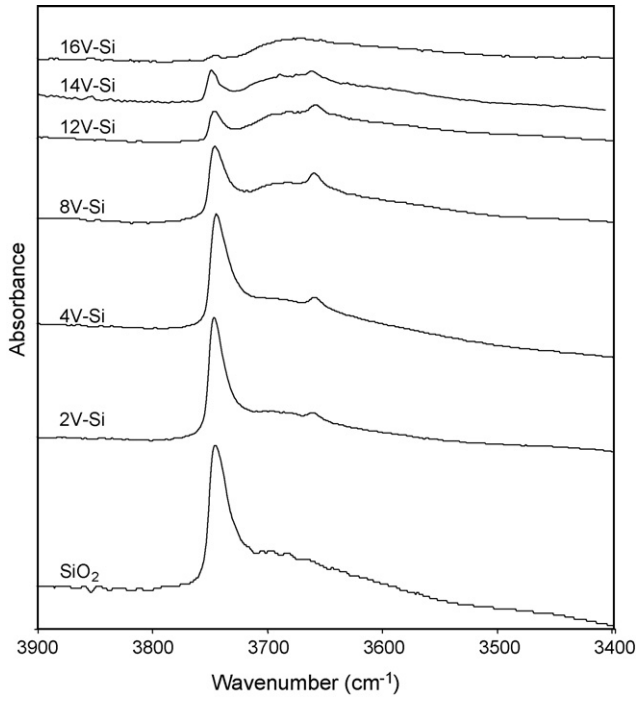

Fig. 3. Infrared O–H stretching region of VO_x/SiO_2 catalysts after re-hydration. Spectra have been normalized on the 805 cm^{-1} silica band. The SiO_2 sample without vanadium was treated under identical conditions as those containing vanadium oxide, guaranteeing that a true comparison can be made between the different catalysts.

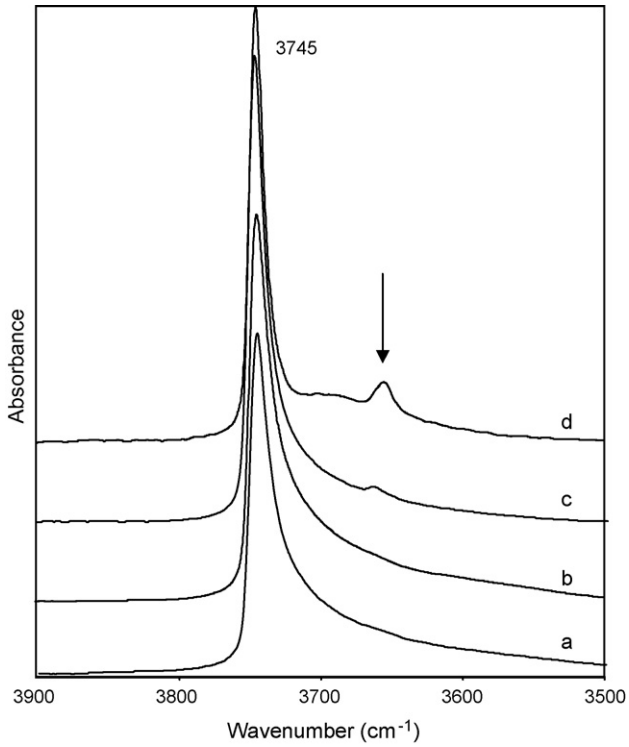

Fig. 4. Raman O–H stretching region of VO_x/SiO_2 catalysts and pure silica. Dehydrated silica (a), dehydrated catalyst 1V–Si (b), rehydrated catalyst 1V–Si (c) and rehydrated catalyst 4V–Si (d). Spectra have been normalized on the 3745 cm^{-1} Si–O–H band.

revealed the band also to be weakly present at lower vanadium oxide loadings. The characteristic V=O stretching Raman band around 1040 cm^{-1} is present in the spectra of all supported vanadium oxide catalysts. At higher loadings (12V–Si and 16V–Si), a second V=O Raman shift appears at 995 cm^{-1} together with bands at 705, 405, 305 and 285 cm^{-1}. These bands are commonly accepted as a fingerprint of crystalline V_2O_5 [25,38,42,48,64,74]. Finally, the Raman spectra of all catalysts exhibit a broad band around 915 cm^{-1}, which is absent in the spectrum of the bare support. The band appears to be unaffected by applying a high vacuum at 700 K for 3 h instead of exposure to a flow of oxygen.

Interestingly, the IR and Raman spectra of the dehydrated samples 2V–Si and 4V–Si, recorded at 77 K in a similar cell as used for the EXAFS measurements, revealed only small differences in the fingerprint area. However, a significant change in the O–H stretching region was observed, very much alike the spectra of the hydrated catalysts shown in Figs. 3 and 4, pointing towards a partial hydroxylation of the catalyst samples.

3.2. Rehydration of samples

Significant changes in the fingerprint region of the IR and Raman spectra were not observed upon admitting ambient air to the dehydrated catalysts. In contrast, the O–H stretching region 3700–3500 cm^{-1} in both the IR (Fig. 3) and Raman spectra (Fig. 4) changed instantaneously. Next to the sharp band at 3745 cm^{-1}, commonly assigned to the free (Si–)O–H stretching vibration of the support [13,39,42,74], a small peak at 3660 cm^{-1} appeared. This peak correlates with the isolated (V–)O–H stretching vibration as reported in literature [40,41,75–77] and is absent in the spectra of the bare support and the fully dehydrated samples. Fig. 3 also illustrates that the relative intensity of the free (Si–)O–H band decreases on increasing vanadium oxide loading, which is in line with the assumption that VO_x anchors on the support by consuming silica hydroxyl groups. The same can be concluded from Fig. 4. After normalization on the (Si–)O–H Raman band, the intensity of the (V–)O–H band of the 4V–Si catalyst is clearly enhanced compared to the one of the 1V–Si sample, which confirms the correlation with the amount of VO_x on the support. The time-resolved IR spectra of the 4V–Si and 8V–Si samples, recorded during the first 30 s after exposure to ambient air (see Fig. 5), reveal that the free (Si–)O–H stretching band at 3745 cm^{-1} remains virtually unaltered during the beginning of the rehydration process. In contrast, the relatively sharp (V–)O–H band at 3660 cm^{-1} and the broad 'support' Si–O–H band around 3680 cm^{-1} on which the V–O–H is superimposed, rapidly gain intensity. The enhancement of the support band and its shift to lower wavenumber is mainly visible in IR, which implies that the corresponding vibration(s) must be subject to hydrogen bonding interactions. This is confirmed by the IR and Raman spectra of the fully hydrated catalysts. As expected, the 'bridged' OH band is practically Raman inactive, whereas, in IR, the band broadens dramatically, increases in intensity and shifts to 3400 cm^{-1}, while the free (Si–)O–H and (V–)O–H

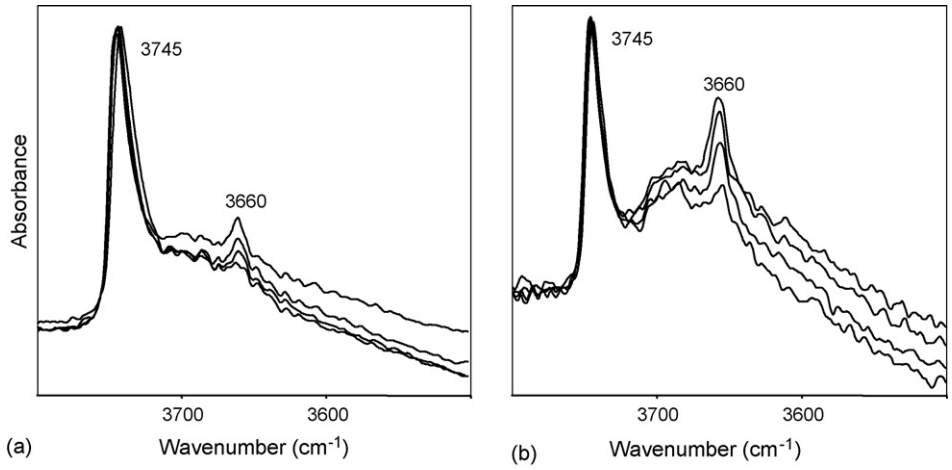

Fig. 5. Time-resolved infrared O–H stretching region of (a) 4V–Si and (b) 8V–Si catalyst. Scans were taken at 2, 10, 20 and 30 s after exposure to ambient air.

bands become relatively weak. Similar observations were made by Nguyen et al. [40]. Upon full rehydration, the IR and Raman fingerprint region revealed the re-appearance of a band at 975 cm^{-1}, which is in accordance with the preceding assignment to a Si–O–H vibration. The Raman spectra as presented in Fig. 6 also showed the presence of a band around 700 cm^{-1}, which is absent in the spectrum of bare hydrated silica. Also, a band at 930 cm^{-1} is present, which is more intense and shifted compared to the 915 cm^{-1} band in the spectra of the dehydrated samples.

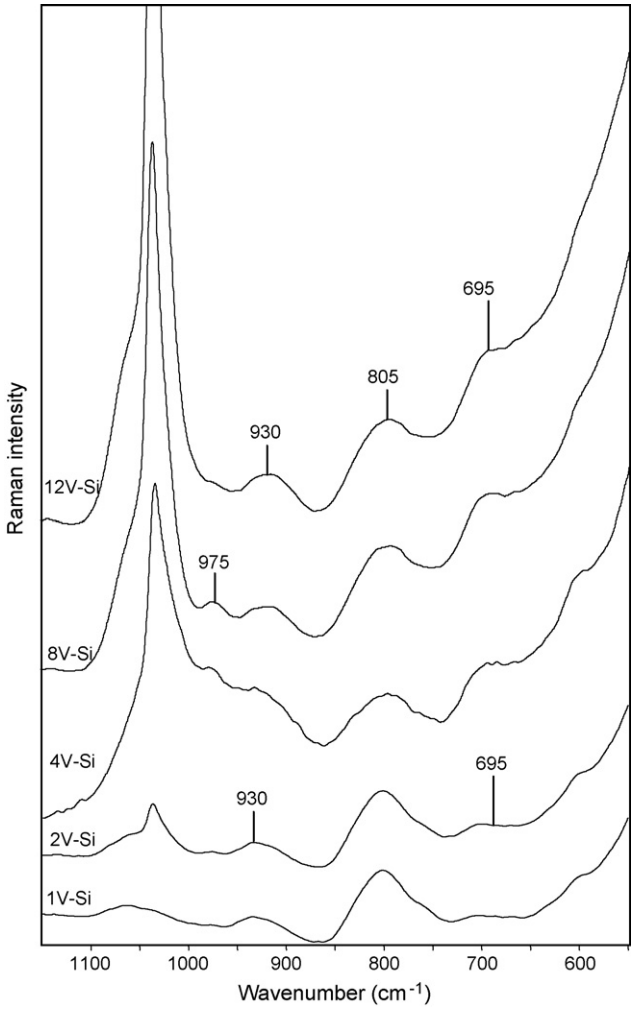

Fig. 6. Raman fingerprint region of fully hydrated VO_x/SiO_2 catalysts recorded at ambient conditions. Spectra have been normalized on the silica band at 805 cm^{-1}.

4. UV–vis spectroscopy

The UV–vis spectra of the dehydrated catalysts with loadings of 1, 4, 12 and 16 wt.% VO_x are shown in Fig. 7. The spectra are dominated by the charge transfer (CT) transition of the type $O^{2-} \rightarrow V^{5+}$ (d^0) with an edge energy of about 3.20 eV (400 nm). According to literature, the onset of the CT transitions exhibit a red shift with increasing vanadium oxide loading [26]. The presence of d–d transitions, typical for the presence of reduced vanadium oxide species is not observed. For the 12V–Si and 16V–Si samples, a shoulder on the low energy side of the CT band is observed, indicating the formation of V_2O_5. Upon rehydration, all supported vanadium oxide catalysts showed a red shift of the CT-band

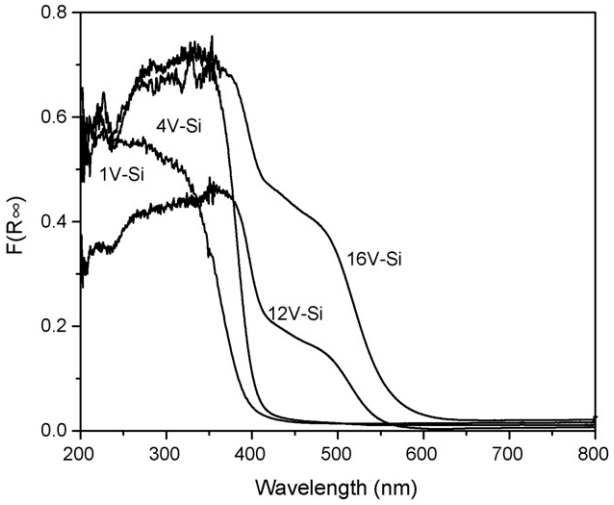

Fig. 7. UV–vis-NIR spectra of dehydrated VO_x/SiO_2 catalysts.

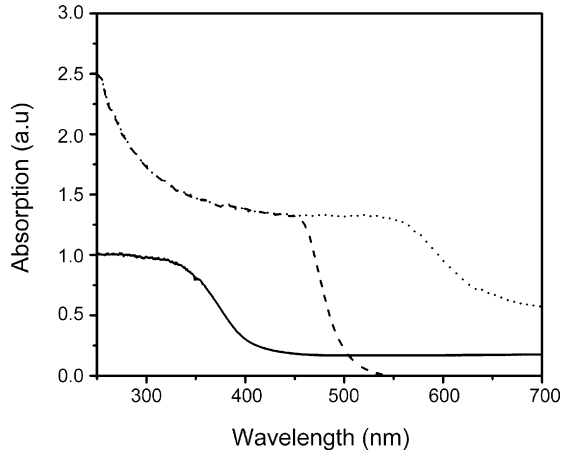

Fig. 8. UV–vis spectra of $[VO(O–O)]^+$ (···), $[VO(O–O)_2]^-$ (– – –), and 1V–Si (—) in aqueous solution.

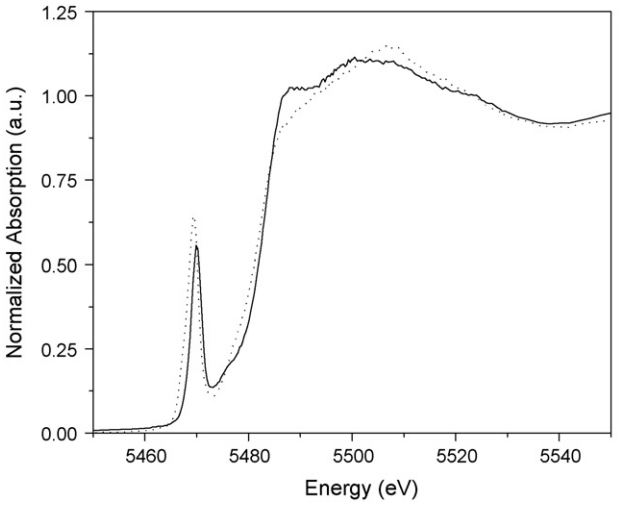

Fig. 9. Vanadium K-edge XANES spectra of dehydrated (solid line) and fully hydrated 1V–Si (dotted line).

edge of about 50–100 nm, depending on the vanadium oxide loading. In order to check the presence of a peroxo ligand, additional spectra were recorded of $[VO(O–O)]^+$ and $[VO(O–O)_2]^-$ ions in aqueous solution (Fig. 8). The characteristic peroxide CT band in the 510–560 nm region is present in the spectra of these compounds, but evidently absent in the spectrum of the 1V–Si sample sample [78].

5. XAFS spectroscopy

The XANES and EXAFS spectra with the corresponding FT's (k^1, Δk = 2–11 Å^{-1}) of the dehydrated and the hydrated 1V–Si catalyst are shown in Figs. 9 and 10. The pre-edge peak (Fig. 9) of the hydrated sample is lower in intensity and the shape of the total edge data is different pointing to another coordination geometry. The pre-edge intensity observed for the dehydrated catalyst is 0.64, indicating that the molecular structure of the vanadium oxide species resembles a distorted tetrahedron [79]. The value observed for the 'wet' sample is 0.52, moving further away from the value for a perfect tetrahedron. Differences are observed for the raw EXAFS data and the corresponding Fourier transforms (see Fig. 10). A comparison of the FT's of dehydrated and fully hydrated shows a lower amplitude, differences around 1.8 Å and a new peak around 2.8 Å. From this can be concluded that hydration has a large influence on the structural properties of the 1V–Si sample. The first two nodes of the imaginary parts of the FT's, however, are remarkably similar. This part of the FT is probably due to a V=O coordination. The EXAFS data-analysis for dehydrated 1V–Si has been reported previously and the coordination geometry of the VO_4 cluster including the structure of the interface between the cluster and the silica support has been investigated [33]. A summary of the fit results is given in Table 2.

The EXAFS data-analysis of the fully hydrated 1V–Si sample was carried out in two consecutive steps. It can be seen in Fig. 9 that a node occurs in the FT of the data around 2.4 Å. It was tried to apply a R-space fit (k^1, Δk = 2.5–11 Å^{-1}, ΔR = 0.7–2.3 Å), which allowed the use of 10.6 fit parameters [80]. A three shell model was applied using a geometry with the following oxygen coordination: $V–O_{(1)}$ (N = 1, R = 1.58 Å), ascribed to the V=O bond, a $V–O_{(2)}$ (N = 3) and $V\cdots O_{(3)}$ (N = 1), both to explain the large differences around 1.8 Å. It was found that the data could be fit besides a V=O coordination at 1.58 Å, with three V–O bonds with 1.83 Å and one oxygen contribution at 2.37 Å. Compared to the dehydrated sample the V–O bonds are longer and an extra oxygen contribution has been introduced, most probably due to the presence of an adsorbed water molecule. Moreover, the FT of the difference file [raw data minus ($V–O_1$ + $V–O_2$ + $V–O_3$)] still

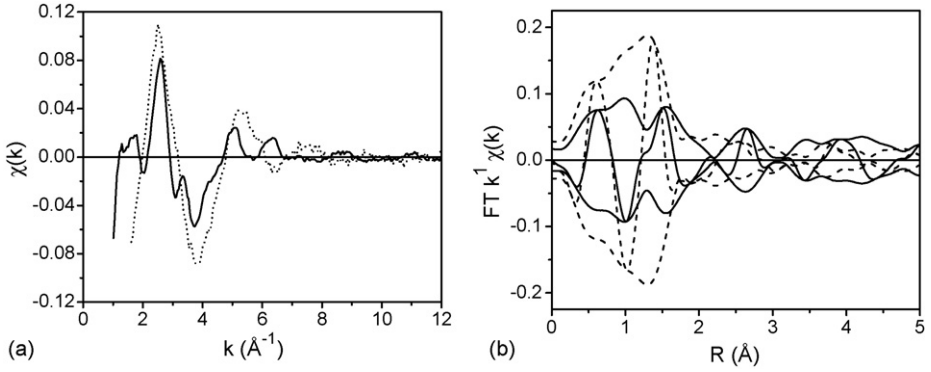

Fig. 10. (a) EXAFS and (b) Fourier transform (k^1, Δk = 2.5–11 Å^{-1}) of dehydrated (solid line) and hydrated 1V–Si (dotted line).

Table 2
Structural parameters from all *R*-space fits of the experimental EXAFS for dehydrated 1V–Si (Δk = 2.5–11 Å^{-1}; ΔR = 0.7–4.0 Å) and total fit (Δk = 2.5–11 Å^{-1}; ΔR = 0.7–4.4 Å) for hydrated 1V–Si

Sample	Scattering pair	N	R (Å)	$\Delta\sigma^2$	ΔE_0	Variances	
						Imaginary part	Absolute part
1V–Si dehydrated	V=O(1)	1.00	1.58	−0.00274	10.76	1.5	1.3
	V–O(2)	3.07	1.77	−0.00156	0.07		
	V···Si(3)	1.06	2.61	0.01500	5.01		
	V···O(4)	2.10	2.70	0.01203	9.88		
	V···Si(5)	0.98	2.95	0.01700	−4.44		
	V···O(6)	1.24	3.28	0.01315	7.15		
	V···O(7)	3.89	3.69	0.01379	−5.14		
1V–Si hydrated	V=O(1)	0.98[a]	1.58[a]	−0.00350	7.68	2.5	1.9
	V–O(2)	3.03[a]	1.83[a]	0.01176	4.86		
	V···O(3)	1.00[a]	2.37[a]	−0.00112	12.35		
	V···O(4)	1.95	2.92	0.00893	−14.35		
	V···Si(5)	1.02	2.93	0.00010	−10.36		
	V···V(6)	1.40	3.18	0.01683	−5.69		
	V···O(7)	4.02	3.82	0.01354	−13.33		

N is the coordination number, R the distance in Å, $\Delta\sigma^2$ the Debye–Waller factor and ΔE_0 is the internal reference energy.
[a] These parameters were fixed during the fitting procedure.

contained strong contributions of higher coordination shells and therefore higher coordination shells were included to gain information about the position of the vanadium species relative to the support material and the coordination of other vanadium atoms in the vicinity of the absorber atom. The final *R*-space fit is shown in Fig. 11 and its fit parameters are listed in Table 2. This fit (k^1, Δk = 2.5–11 Å^{-1}, ΔR = 0.7–4.4 Å) has been applied with seven coordination shells for which 7 × 4 = 28 fit parameters are needed. The number of allowed independent parameters is 22, calculated according to the Nyquist theorem [80]. Since the number of allowed fit parameters is not infinite, we kept the coordination numbers and inter atomic distances obtained from the three-shell fit constant. The CERIUS 2 structural model was used interactively during the fit process to verify possibly coordinating atoms obtained from our fit. The final fit obtained in this way revealed the variances of the *R*-space fit to be acceptable and lower than 3% (Table 2). A V···V coordination at 3.18 Å with

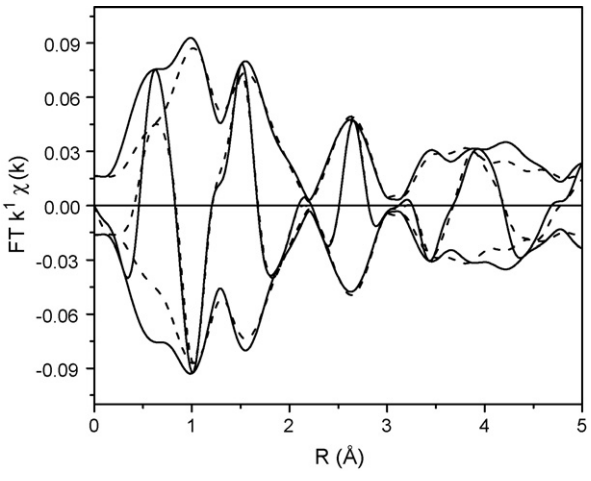

Fig. 11. Fourier transform (k^1, Δk = 2.5–11 Å^{-1}) of raw EXAFS data (—) and total fit with seven shells (- - -) for 1V–Si-hydrated.

average coordination number N = 1.4 had to be included in the fit in contrast to the dehydrated sample [33]. This V···V coordination was introduced to account for the new peak around 2.8 Å, which is most probably due to V complex formation after hydration as mentioned in Section 1. Furthermore, a V···Si coordination was detected at 2.9 Å, almost 0.3 Å longer as detected in the dehydrated sample and several V···$O_{support}$ coordinations had to be included in the fit [32]. All contributions appeared to be well above the noise level.

6. Discussion

Time-resolved IR and Raman spectroscopy convincingly demonstrate that hydroxylation of dehydrated VO_x/SiO_2 catalysts starts with the formation of V–O–H bonds. This is characterized by the instantaneous appearance of a (V–)O–H stretching band around 3660 cm^{-1}. The high frequency of this band, the small bandwidth and the activity in both IR and Raman, indicate that the vibration is 'free' and not subject to hydrogen bonding. At low loadings, the intensity of the (V–)O–H Raman band increases more or less proportional to vanadium oxide loading. In accordance with Nguyen et al. [40], it implies that the band can be used to estimate the amount of VO_x on the support. The appearance of a broad IR band around 3400 cm^{-1} together with the (V–)O–H can be attributed to the formation of bridged Si–O–H bonds. The fact that this occurs within seconds after exposure to air illustrates the high sensitivity to water even at temperatures of 700 K. The decreasing intensity of the free (Si–)O–H stretching band upon increasing the vanadium oxide loading in the IR and Raman spectra confirms that VO_x anchors on the support by consuming silica surface hydroxyl groups. *Vice versa* the (Si–)O–H band intensity increases upon re-hydration, which points to hydroxylation of Si–O–V bonds. The same conclusion can be derived from the IR and Raman band around 975 cm^{-1}. The band is also present in the spectrum

of pure dehydrated silica and is generally assigned to a Si–O(H) stretching vibration [37,38,42,81,82]. Obviously, the band intensity not only decreases with increasing vanadium oxide loading and upon dehydration, but also (partly) re-appears upon hydroxylation. In our opinion, the simultaneous appearance of (V–)O–H and bridged (Si–)O–H and Si–O(H) bands illustrate the conversion of the dehydrated species (b) to the molecular structures (d) and/or (e). However, neither the vibrational data nor the UV–vis results allow to distinguish between these two hydroxylated molecular structures.

The characteristic V=O Raman band around 1040 cm^{-1} reflects the presence of VO_x species in both the hydrated and dehydrated catalysts. The position shifts from 1039 cm^{-1} for the (monomeric) 1V–Si sample to 1046 cm^{-1} for the 8, 12 and 16 wt.% VO_x/SiO_2 catalysts in the dehydrated state. In accordance with literature [48], the position in the hydrated samples shows a small red-shift to 1036 cm^{-1}. The relative intensity seems unaffected. It follows that hydroxylation occurs *via* breaking of Si–O–V bonds.

The IR spectra of the dehydrated compounds show a broad band at 945 cm^{-1}, particularly at high loadings (8–16 wt.%). Spectral subtraction of the support spectrum revealed the band also to be weakly present at lower vanadium oxide loadings, giving support for the literature assignment to a V–O–Si vibration [55,56,81,82]. A relative decrease of the IR band intensity upon re-hydration would have supplied additional evidence for the correctness of this assignment, but unfortunately, the band was obscured by the enhanced intensity of the interfering support Si–O stretching band around 1000 cm^{-1}.

The assignment of the band at 915 cm^{-1} in the Raman spectra of all dehydrated catalysts remains a point of dispute. Various spectral assignments have been given in literature such as a V=O stretch in a polymeric vanadium oxide chain [17,23,42,48,83], but also to a polymeric V–O–V vibration [7]. Other proposals are a V–O–H deformation vibration [49], perturbed Si–O– and Si(–O–)$_2$ modes as result of the anchoring of the vanadium oxide [38,84] and protonated $>V(=O)_2$ and $-V(=O)_3$ vibrations, implying the number of V–O-support bonds to be less than 3 [49]. Recently, Gijzeman et al. [57] suggested that the band might originate from a peroxo O–O stretching vibration, and hence proposed the umbrella geometry (c) as a viable alternative for the more commonly accepted pyramidal form (b). This idea was further elaborated in a recent paper by Van Lingen et al. [58] in which theoretical models (b) and (c) have been compared. It was shown that the umbrella model (c) can be described as a chemisorbed V=O(O_2) species with three oxygen atoms pointing away from the silica surface. The results from DFT calculations on model (c) were found to be consistent with the experimental Raman and EXAFS data and could explain the thermal dependencies of the Raman intensities. Furthermore, the broadness of the 915 cm^{-1} Raman band was attributed to thermal movement of the bound oxygen molecule. Most papers in the literature, however, suggest a Raman band in this area to be a V–O-support vibration [55,56,67,81,82,85–89]. Our data of the dehydrated catalysts show that the Raman band at 915 cm^{-1} is present at all vanadium oxide loadings, and since the EXAFS results exclude di- or polymeric species, this eliminates the spectral assignment to a V–O–V vibration. Also, a (V–)O–H stretching band at 3660 cm^{-1} is absent under severe dehydrated conditions, which excludes the spectral assignment to a V–O–H bending. Furthermore, the 915 cm^{-1} band remains unaffected at 700 K under vacuum. However, according to literature, solid phase vanadium peroxo compounds are thermally unstable and dissociate between 473 and 573 K [90]. This makes that the peroxide O–O stretching vibration as origin of the 915 cm^{-1} band remains at least questionable and additional experimental and theoretical data should be obtained to allow further support for this assignment. The UV–vis data presented in this paper provide further evidence for this conclusion, as a peroxide CT band is experimentally not observed. As a consequence, we revoke based on the current experimental data the proposal of the umbrella structure (c) and conclude that monomeric VO_x species are most likely pyramidal anchored on the silica surface under strictly dehydrated conditions. This geometry (b) would also explain the presence of two Si–O–V interface modes, *i.e.*, an IR active in-phase vibration at 950 cm^{-1} and a Raman active out-of-phase one at 915 cm^{-1}. At first glance, the EXAFS results, pointing to a single V–O–Si bond for the dehydrated 1V–Si sample, are not consistent with this conclusion. However, EXAFS measurements reported in this study as well as in two earlier papers [32,33], were carried out at 77 K which implies that condensation of water, resulting in (partly) hydroxylation of dehydrated VO_4, might very well have occurred. Regarding the extreme sensitivity of the dehydrated catalysts for water, as shown by the vibrational data in this paper, this seemed very plausible. Indeed, the IR and Raman spectra of the 2V–Si and 4V–Si samples, recorded at 77 K in the same cell and under the same conditions as used for EXAFS measurements, confirmed that hydroxylation had occurred with the catalyst samples under investigation. In our opinion, this also explains the presence of a V–O–H band in the IR spectra of assumed dehydrated VO_x/SiO_2 catalysts reported previously in the literature [40]. Presumably, traces of water have been present during the oxidation treatment. As a consequence, the spectral assignment of the 915 cm^{-1} band to a Si–O–V vibration is the most plausible one. Next, upon hydration, the band should reduce in intensity due to the conversion of Si–O–V bonds into V–O–H and Si–O–H. Indeed, one could argue that the band is no longer visible in the Raman spectra and that a slightly more intense band at 930 cm^{-1} appears. Regarding these differences, we assume that the 930 cm^{-1} band either originates from the Si–O–V interface mode of the single anchored structure (e) or from another vibration, possibly a V–O–H bending mode [91,92]. From this discussion, we conclude that the molecular structure of supported vanadium oxide catalysts at low loadings consists only exclusively of structure (b) under severe dehydrated conditions. However, upon exposure to water, conversion to structure (e) occurs almost immediately. Most likely, this process proceeds *via* intermediate (d), but unfortunately, the time-resolved IR and Raman data do not supply conclusive evidence on the presence of this molecular structure. Also on the basis of our EXAFS analysis we cannot exclude the formation of structure (d) since EXAFS is not sensitive towards a minor species present in the recorded spectra.

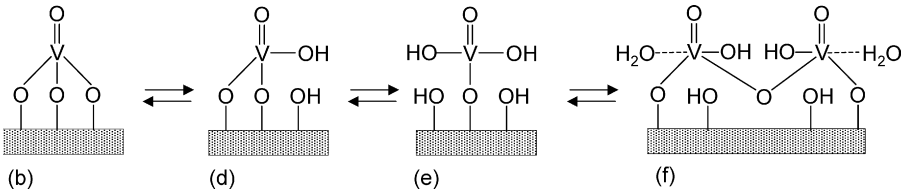

Fig. 12. Schematic dehydration/rehydration mechanism for supported vanadium oxide catalysts. The reaction partner, H_2O, in these surface reactions has not been included in the scheme for simplicity. The last case (f) is formed out of two VO_x units (e) by condensation of two V–OH groups resulting in the formation of a V–O–V bond and H_2O.

At this point, it should be noted that both structures (d) and (e) could be important vanadium oxide species under reaction conditions if traces of water are formed as reaction product, *e.g.*, in the selective oxidation of methanol to formaldehyde and the oxidative dehydrogenation of alkanes. Depending on the water vapor pressure, reaction temperature and hydroxylation degree of the support oxide, structure (e) could be even the dominant vanadium oxide species under reaction conditions.

Finally, the Raman spectra of the fully hydrated catalysts also showed a band around 700 cm^{-1}, absent in the spectra of the dehydrated catalyst samples and silica. The absence of bands at 995, 405, 305 and 285 cm^{-1} excludes the presence of crystalline V_2O_5. However, a band at ~700 cm^{-1} is weakly present in the spectrum of dehydrated 8V–Si where polymeric species are assumed to be present. Therefore, we assign the band to a V–O–V vibration of di- or polymeric species [38,55,56]. This conclusion is supported by the results from EXAFS analysis. Fitting of the fully hydrated 1-V–Si sample showed the necessity to introduce a V···V coordination to account for a peak around 2.8 Å, in the non-phase corrected Fourier transform. The origin of this peak can only be explained by the formation of larger clusters such as dimeric V_2O_7 as predicted on the basis of the low pH at PZC for silica supports. Besides, a V···Si coordination was detected at 2.9 Å, which is almost 0.3 Å longer as detected in the dehydrated 1V–Si sample, further illustrating the effects of water on the local vanadium oxide structure on an oxidic support.

7. Conclusions

Summarizing all observations, we conclude that dehydrated silica-supported VO_x catalysts are extremely reactive to water vapor. Upon exposure to traces of H_2O, partial hydroxylation instantaneously occurs, which is characterized by the appearance of a (V–)O–H stretching band in both the IR and Raman spectra. The Raman spectra of the dehydrated samples are unaffected by high temperature and vacuum, implying that the assignment of an O–O stretching vibration is questionable. Hence, it is unsure if the peroxo structure (c) really exists on a catalyst surface under the conditions described in this work. This conclusion is further evidenced by the corresponding UV–vis data. As a consequence, it is concluded that dehydrated monomeric VO_4 species are pyramidal anchored at the silica surface and that the corresponding molecular structure (b) is converted to the hydroxylated umbrella-type species (e) upon exposure to H_2O. It is reasonable to assume that the conversion proceeds via molecular structure (d), but experimental evidence for this hypothesis could not be found. The fact that the EXAFS data of the assumed dehydrated 1V–Si catalyst point to only one V–O–Si bond can be attributed to hydroxylation of the catalyst material due to condensation effects at 77 K in the measuring cell. IR and Raman measurements of the 2V–Si and 4V–Si catalysts under the same experimental conditions confirmed that the vanadium oxide species were partially hydrated under these circumstances.

The appearance of a V–O–V vibration at 700 cm^{-1} in the Raman spectra of the hydrated compounds suggests the formation of di- or polymeric species as result of further rehydration. EXAFS analysis supports this conclusion, since V atoms are detected at ~3.2 Å, showing the formation of larger vanadium oxide clusters upon total hydration even for a low V loading of 1 wt.%. The hydrated VO_x species are attached to the surface with one V–O–Si bond, but the oxygen coordination changes from four to five atoms. The latter points to the physisorption of a water molecule at ~2.35 Å. As a result we propose a model for a stepwise hydration mechanism of pyramidal anchored monomeric VO_x species on a silica support as schematically depicted in Fig. 12. The hydration mechanism, proposed on the basis of our measurements, is in line with the mechanism previously reported in literature by, *e.g.*, Wachs and co-workers [38]. In both cases stepwise hydration of the V–O–Si bonds is followed by the formation of larger vanadium oxide clusters. Regarding the extreme sensitivity of the dehydrated species, it is plausible to assume that different molecular structures of VO_x will be present under realistic reaction conditions. Finally, we would like to stress the importance of combining IR, Raman, UV–vis and EXAFS spectroscopy, or any other combination of complementary spectroscopic techniques in general. As demonstrated, the complementary information from spectroscopic techniques, particularly when obtained under identical experimental conditions, allows elucidation of the molecular structure of silica supported vanadium oxide catalysts. Besides, it appears to be crucial to prevent incorrect interpretations and to assess potential differences in the applied measuring conditions, particularly when different in situ cells have to be used.

Acknowledgments

The EXAFS work at the HASYLAB beam station was supported by the IHP-contract HPRI-CI-2001-00140 of the European Commission. BMW acknowledges financial support from NRSCC, NWO/CW-Van der Leeuw, NWO/CW-VICI and a EU-COST D15 program.

References

[1] B.M. Weckhuysen, D.E. Keller, Catal. Today 78 (2003) 25.
[2] J.M. López Nieto, P. Concepción, A. Dejoz, H. Knozinger, F.V. Melo, M.I. Vazquez, J. Catal. 189 (2000) 147.
[3] K. Wada, Y. Yamada, E. Watanabe, T. Mitsudo, J. Chem. Soc., Faraday Trans. 94 (1998) 1771.
[4] Z.P. Zhu, Z.Y. Liu, S.J. Liu, H.X. Niu, Appl. Catal. B: Environ. 23 (1999) 229.
[5] H. Bosch, F.J.J.G. Janssen, F.M.G. Van den Kerkhof, J. Oldenziel, J.G. Van Ommen, J.R.H. Ross, Appl. Catal. 25 (1986) 239.
[6] M.D. Amiridis, I.E. Wachs, G. Deo, J.-M. Jehng, D. Soung Kim, J. Catal. 161 (1996) 247.
[7] L.J. Burcham, G. Deo, X. Gao, I.E. Wachs, Top. Catal. 11/12 (2000) 85.
[8] P. Concepción, B.M. Reddy, H. Knözinger, Phys. Chem. Chem. Phys. 1 (1999) 3031.
[9] L.J. Burcham, L.E. Braind, I.E. Wachs, Langmuir 17 (2001) 6164.
[10] K. Hadjiivanov, P. Concepción, H. Knozinger, Top. Catal. 11 (2000) 123.
[11] I.E. Wachs, Colloid Surf. 105 (1995) 143.
[12] M.A. Centeno, I. Carrizosa, J.A. Odriozola, Appl. Catal. B: Environ. 29 (2001) 307.
[13] G. Martra, F. Arena, S. Coluccia, F. Frusteri, A. Parmaliana, Catal. Today 63 (2000) 197.
[14] N.-Y. Topsøe, Science 265 (1994) 1217.
[15] T.J. Dines, C.H. Rochester, A.M. Ward, J. Chem. Soc., Faraday Trans. 87 (1991) 1617.
[16] I.E. Wachs, J.-M. Jehng, G. Deo, B.M. Weckhuysen, V.V. Guliants, J.B. Benziger, S. Sundaresan, J. Catal. 170 (1997) 75.
[17] U. Scharf, M. Schraml-Marth, A. Wokaun, A. Baiker, J. Chem. Soc., Faraday Trans. 87 (1991) 3299.
[18] F. Hatayama, T. Ohno, T. Marouka, T. Ono, H. Miyata, J. Chem. Soc., Faraday Trans. 87 (1991) 2629.
[19] A. Burkhardt, W. Weisweiler, J.A.A. Van den Tillaart, A. Shafer-Sindlinger, E.S. Lox, Top. Catal. 16 (2001) 369.
[20] B. Olthof, A. Khodakov, A.T. Bell, E. Iglesia, J. Phys. Chem. B 104 (2000) 1516.
[21] D.A. Bulushev, L. Kiwi-Minsker, F. Rainone, A. Renken, J. Catal. 205 (2001) 115.
[22] I.E. Wachs, G. Deo, M. Vuurman, H. Hu, D. Soung Kim, J.-M. Jehng, J. Mol. Catal. 82 (1993) 443.
[23] M.A. Vuurman, I.E. Wachs, J. Phys. Chem. 96 (1992) 5008.
[24] I.E. Wachs, Top. Catal. 8 (1999) 57.
[25] X. Gao, M.A. Bañares, I.E. Wachs, J. Catal. 188 (1999) 325.
[26] X. Gao, I.E. Wachs, J. Phys. Chem. B 104 (2000) 1261.
[27] B.M. Weckhuysen, I.P. Vannijvel, R.A. Schoonheydt, Zeolites 15 (1995) 482.
[28] E.V. Kondratenko, M. Baerns, Appl. Catal. A: Gen. 222 (2001) 133.
[29] K. Tran, M.A. Hanning-Lee, A. Biswas, A.E. Stiegman, G.W. Scott, J. Am. Chem. Soc. 117 (1995) 2618.
[30] M. Ruitenbeek, F.M.F.d. Groot, A.J.V. Dillen, D.C. Koningsberger, Stud. Surf. Sci. Catal. D 130 (2000) 3101.
[31] M. Ruitenbeek, A.J. van Dillen, F.M.F. de Groot, I.E. Wachs, J.W. Geus, D.C. Koningsberger, Top. Catal. 10 (2000) 241.
[32] D.E. Keller, F.M.F. de Groot, D.C. Koningsberger, B.M. Weckhuysen, J. Phys. Chem. B 109 (2005) 10223.
[33] D.E. Keller, D.C. Koningsberger, B.M. Weckhuysen, J. Phys. Chem. B 110 (2006) 14313.
[34] T. Okuhara, K. Inumaru, M. Misono, N. Matsubayashi, H. Shimada, A. Nishijima, Catal. Lett. 20 (1993) 73.
[35] K. Inumaru, M. Misono, T. Okuhara, Appl. Catal. A: Gen. 149 (1997) 133.
[36] G. Silversmit, J.A. van Bokhoven, H. Poelman, A.M.J. van der Eerden, G.B. Marin, M.-F. Reyniers, R. De Gryse, Appl. Catal. A: Gen. 285 (2005) 151.
[37] J.-M. Jehng, G. Deo, B.M. Weckhuysen, I.E. Wachs, J. Mol. Catal. A: Chem. 110 (1996) 41.
[38] X. Gao, S.R. Bare, B.M. Weckhuysen, I.E. Wachs, J. Phys. Chem. B 102 (1998) 10842.
[39] H. Berndt, A. Martin, A. Brückner, E. Schreier, D. Müller, H. Kosslick, G.U. Wolf, B. Lücke, J. Catal. 191 (2000) 384.
[40] L.D. Nguyen, S. Loridant, H. Lanay, A. Pigamo, J.L. Dubois, J.M.M. Millet, J. Catal. 237 (2006) 38.
[41] P. Van Der Voort, M.G. White, M.B. Mitchell, A.A. Verberckmoes, E.F. Vansant, Spectrochim. Acta A 53 (1997) 2181.
[42] M. Schraml-Marth, A. Wokaun, M. Pohl, H.-L. Krauss, J. Chem. Soc., Faraday Trans. 87 (1991) 2635.
[43] S. Dzwigaj, E.M. El Maki, M.J. Peltre, P. Massiani, A. Davidson, M. Che, Top. Catal. 11/12 (2000) 379.
[44] M.F. Hazenkamp, G. Blasse, J. Phys. Chem. 96 (1992) 3442.
[45] S. Yoshida, T. Tanaka, T. Hanada, T. Hiraiwa, H. Kanai, T. Funabiki, Catal. Lett. 12 (1992) 277.
[46] U.G. Nielsen, N.-Y. Topsoe, M. Brorson, J. Skibsted, H.J. Jakobsen, J. Am. Chem. Soc. 126 (2004) 4926.
[47] M. Ruitenbeek, Characterisation of vanadium-based oxidation catalysts, Thesis, Utrecht University, 1999.
[48] G.T. Went, S.T. Oyama, A.T. Bell, J. Phys. Chem. 94 (1990) 4240.
[49] G. Deo, I.E. Wachs, J. Haber, Crit. Rev. Surf. Chem. 4 (1994) 141.
[50] C.F. Baes, R.E. Mesmer, The Hydrolysis of Cations, John Wiley & Sons, New York, 1976, pp. 210.
[51] M.A. Bañares, I.E. Wachs, J. Raman Spectrosc. 33 (2002) 359.
[52] G. Deo, I.E. Wachs, J. Phys. Chem. 95 (1991) 5889.
[53] B.M. Weckhuysen, I.E. Wachs, in: H.S. Nalwa (Ed.), Handbook of Surfaces and Interfaces of Materials, vol. 1, Academic Press, San Diego, 2001, p. 613.
[54] A. Khodakov, B. Olthof, A.T. Bell, E. Iglesia, J. Catal. 181 (1999) 205.
[55] N. Magg, J.B. Giorgi, T. Schroeder, M. Bäumer, H.-J. Freund, J. Phys. Chem. B 106 (2002) 8756.
[56] N. Magg, B. Immaraporn, J.B. Giorgi, T. Schroeder, M. Baumer, J. Dobler, Z. Wu, E. Kondratenko, M. Cherian, M. Baerns, P.C. Stair, J. Sauer, H.-J. Freund, J. Catal. 226 (2004) 88.
[57] O.L.J. Gijzeman, J.N.J. van Lingen, J.H. van Lenthe, S.J. Tinnemans, D.E. Keller, B.M. Weckhuysen, Chem. Phys. Lett. 397 (2004) 277.
[58] J.N.J. Van Lingen, O.L.J. Gijzeman, B.M. Weckhuysen, J.H. Van Lenthe, J. Catal. 239 (2006) 34.
[59] G. Busca, G. Centi, L. Marchetti, F. Trifiro, Langmuir 2 (1986) 568.
[60] B.M. Weckhuysen, J.-M. Jehng, I.E. Wachs, J. Phys. Chem. B 104 (2000) 7382.
[61] G. Busca, J. Raman Spectrosc. 33 (2002) 348.
[62] I.E. Wachs, Catal. Today 27 (1996) 437.
[63] S. Takenaka, T. Tanaka, T. Yamazaki, T. Funabiki, S. Yoshida, J. Phys. Chem. B 101 (1997) 9035.
[64] S.T. Oyama, G.T. Went, K.B. Lewis, A.T. Bell, G.A. Somorjai, J. Phys. Chem. 93 (1989) 6786.
[65] H. Eckert, I.E. Wachs, J. Phys. Chem. 93 (1989) 6796.
[66] L.R. Le Coustumer, B. Taouk, M. Le Meur, E. Payen, M. Guelton, J. Grimblot, J. Phys. Chem. 92 (1988) 1230.
[67] Z. Wu, H.-S. Kim, P.C. Stair, S. Rugmini, S.D. Jackson, J. Phys. Chem. B 109 (2005) 2793.
[68] B.M. Weckhuysen, L.M. de Ridder, R.A. Schoonheydt, J. Phys. Chem. 97 (1993) 4756.
[69] B.M. Weckhuysen, R.A. Schoonheydt, Catal. Today 49 (1999) 441.
[70] F.W.H. Kampers, T.M.J. Maas, J. van Grondelle, P. Brinkgreve, D.C. Koningsberger, Rev. Sci. Instrum. 60 (1989) 2635.
[71] M. Vaarkamp, J.C. Linders, D.C. Koningsberger, Phys. B 208/209 (1995) 159.
[72] M. Vaarkamp, J.C. Linders, D.C. Koningsberger, Phys. B 208/209 (2000) 143.
[73] CERIUS 2, 3.5 ed., Molecular Simulations Inc., San Diego, 1997.
[74] M. Baltes, K. Cassiers, P. Van der Voort, B.M. Weckhuysen, R.A. Schoonheydt, E.F. Vansant, J. Catal. 197 (2001) 160.
[75] A. Davydov, Molecular Spectroscopy of Oxide Catalyst Surfaces, John Wiley & Sons, Chicester, UK, 2003.
[76] M.N. Kantcheva, K. Hadjiivanov, D.G. Klissurski, I. Konstantin, J. Catal. 134 (1992) 299.
[77] M.N. Kantcheva, Solid State Ionics 141/142 (2001) 487.

[78] M. Vennat, J.-M. Brégeault, P. Herson, Dalton Trans. (2004) 908.
[79] J. Wong, F.W. Lytle, R.P. Messmer, D.H. Maylotte, Phys. Rev. B 30 (1984) 5596.
[80] E.A. Stern, Phys. Rev. B 48 (1993) 9825.
[81] G.L. Rice, S.L. Scott, J. Mol. Catal. A: Chem. 125 (1997) 73.
[82] G.L. Rice, S.L. Scott, Langmuir 13 (1997) 1545.
[83] G.T. Went, L.-J. Leu, A.T. Bell, J. Catal. 134 (1992) 479.
[84] X. Gao, S.R. Bare, J.L.G. Fierro, M.A. Bañares, I.E. Wachs, J. Phys. Chem. B 102 (1998) 5653.
[85] R. Rulkens, J. Male, L.K.W. Terry, B. Olthof, A. Khodakov, A.T. Bell, E. Iglesia, T.D. Tilley, Chem. Mater. 11 (1999) 2966.
[86] V. Brázdová, M.V. Ganduglia-Pirovano, J. Sauer, Phys. Rev. B 69 (2004) 165420.
[87] Y. Segura, P. Cool, P. Kustrowski, L. Chmielarz, R. Dziembaj, E.F. Vansant, J. Phys. Chem. B 109 (2005) 12071.
[88] Z. Wu, P.C. Stair, J. Catal. 237 (2006) 220.
[89] C. Moisii, M.D. Curran, L.J. van de Burgt, A.E. Stiegman, J. Mater. Chem. 15 (2005) 3519.
[90] D. Joniaková, P. Schwendt, Thermochim. Acta 92 (1985) 701.
[91] P.G. Dickens, A.M. Chippindale, S.J. Hibble, P. Lancaster, Mater. Res. Bull. 19 (1984) 319.
[92] T. Hirata, K. Yagisawa, J. Alloys Compd. 185 (1992) 177.